DEFENCE R&D DÉFENSE

Shoreline Mapping Using Interferometric SAR

Karim E. Mattar, Max Buchheit and André Beaudoin

Defence R&D Canada
TECHNICAL REPORT
DREO TR 2001-078
October 2001

National Defence Défense nationale

Canada

Abstract

Coherence from repeat-pass Satellite Radar Interferometry (SRI) is explored as a means for shoreline mapping and water body masking. In temperate environments, the coast may be outlined by the difference between the high coherence of the land and the absence of coherence in the sea/ocean. However, it is found that in coastal regions scene decorrelation from a variety of sources often dominates the image, making it difficult or impossible to distinguish the shoreline. In an arctic climate where scene decorrelation is reduced and the sea is frozen, the shoreline is often clearly outlined by a thin region of low coherence separating the land from frozen ice that is subjected to continuous tidal shear forces. Lakes are similarly outlined by a higher phase noise and consequently lower coherence.

Résumé

On étudie la possibilité d'utiliser la cohérence de l'interférométrie radar par satellite à passage répété comme outil pour la cartographie du littoral et le masquage de plans d'eau. Dans les milieux tempérés, la côte peut être définie par la différence entre la cohérence élevée de la terre et l'absence de cohérence de la mer (océan). Cependant, on constate que dans les régions côtières la décorrélation de la scène attribuable à une variété de sources est souvent dominante dans l'image, ce qui rend la distinction du littoral difficile ou impossible. Dans un environnement arctique, où la décorrélation de la scène est réduite et où la mer est glacée, le littoral est souvent défini de façon nette par une étroite région de faible cohérence séparant la terre de la glace qui subit des forces de cisaillement continuelles dues aux marées. Les lacs sont définis de façon similaire par un bruit de phase supérieur et par conséquent une cohérence inférieure.

This page intentionally left blank.

Executive summary

J2 Geomatics and The National Imagery and Mapping Agency (NIMA), USA, are taking advantage of recent advances in remote sensing technologies to improve their vector shoreline database. Accurate water-body masking is also a central issue in the generation of topographic maps to NIMA standards. This coincides with the NIMA sponsored single-pass interferometric Shuttle Radar Topographic Mission (SRTM) designed to map 85% of the earth's land surface (between the latitudes of ±60°) to DTED level 2 accuracy. J2 Geomatics has also undertaken to explore mapping the Canadian territory north of 60° to these same standards.

In 1998 a project was initiated between the Defence Research Establishment Ottawa (DREO) and NIMA to study shoreline extraction from radar backscatter and radar polarimetry. In this report we explore the use of satellite repeat-pass interferometry (SRI) to the same end.

Interferometry is one of the most significant tools to have evolved from Synthetic Aperture Radar (SAR) in recent years. Single and repeat-pass Interferometric SAR (InSAR) are both being used for topographic mapping. The phase difference and correlation between the InSAR pair (also known as the coherence) are also being used for a wide range of applications.

The coherence varies greatly with the environment. In temperate environments, the shoreline is ideally defined by the interface between the relatively high coherence of the shore and the absence of coherence from the body of water. In practice, scene decorrelation from a variety of sources reduces, and often completely eliminates, coherence along the shore, thereby severely limiting the visibility of the shoreline in coherence maps.

The use of coherence for shoreline mapping and water body masking, holds much more promise in arctic environments where decorrelation is minimised and the frozen water bodies and (frozen) land generally maintain a high coherence for a prolonged period of time. Under these circumstances the coastline is often clearly outlined by a thin shear region of low coherence separating the two regions of higher coherence. This shear region is formed by the tidal induced change in the level of the sea ice relative with the land. The large volume component of the scattering from Lake Ice results in the degradation in the coherence of the lake, which contrast well with, and can often be easily separated from, the higher coherence of the surrounding land.

The very requirement of a sampling window of pixels to estimate the coherence, limits, and indeed lowers, the coherence map's resolution relative to the inherent resolution of the radar backscatter image. This disadvantage can be addressed by varying the size and shape of the estimation window, by using multi-resolution coherence maps, by supplementing the coherence map with the readily available higher resolution radar backscatter image, interferogram phase, or residue images, or by use of a multi-temporal approach.

Mattar, K., Buchheit, M., Beaudoin, A., 2001, Shoreline Mapping Using Interferometric SAR, DREO TR 2001-078, Defence Research Establishment Ottawa

Sommaire

J2 Géomatique et la National Imagery and Mapping Agency (NIMA) des É.-U. profitent des perfectionnements récents des technologies de télédétection pour améliorer leur base de données vectorielles sur le littoral. Le masquage précis de plans d'eau constitue aussi un élément clé de la production de cartes topographiques conformes aux normes de la NIMA. Cette activité coïncide avec la mission de cartographie radar interférométrique de la navette (Shuttle Radar Topographic Mission - SRTM) à passage unique financée par la NIMA et destinée à cartographier 85 % de la surface continentale de la Terre (entre les latitudes +60° et -60°) jusqu'à une précision de niveau 2 des données de relief numériques (DTED). J2 Géomatique a aussi commencé à étudier la possibilité de cartographier le territoire canadien au nord de la latitude 60° conformément aux mêmes normes.

En 1998, un projet a été mis sur pied conjointement par le Centre de recherches pour la défense Ottawa (CRDO) et la NIMA en vue d'étudier la possibilité de définir le littoral à partir de la rétrodiffusion radar et de la polarimétrie radar. Dans le présent rapport, nous étudions la possibilité d'utiliser dans le même but l'interférométrie par satellite à passage répété (SRI).

L'interférométrie est un des outils les plus précieux obtenu grâce au radar à antenne synthétique (SAR) ces dernières années. Le SAR interférométrique (InSAR) à passage unique et le SAR interférométrique à passage répété sont tous deux utilisés pour la cartographie topographique. La différence de phase et la corrélation entre les deux InSAR de la paire (qu'on appelle aussi la cohérence) sont également utilisées dans une vaste gamme d'applications.

La cohérence varie grandement selon le milieu. Dans les milieux tempérés, le littoral est défini de façon idéale par l'interface entre la cohérence relativement élevée du rivage et l'absence de cohérence du plan d'eau. En pratique, la décorrélation de la scène attribuable à une variété de sources réduit, et souvent élimine entièrement, la cohérence le long du rivage, ce qui limite fortement la visibilité du littoral sur les cartes de cohérence.

L'utilisation de la cohérence pour la cartographie du littoral et le masquage des plans d'eau est beaucoup plus prometteuse pour les milieux arctiques, où la décorrélation est réduite et où les plans d'eau glacés et le sol (gelé) donnent généralement une cohérence élevée pendant une longue période. Dans ces conditions, la ligne de côte est souvent définie de façon nette par une étroite région de cisaillement de faible cohérence séparant deux régions de cohérence plus élevée. Cette région de cisaillement est créée par les variations du niveau de la glace de mer par rapport à la terre dues aux marées. La composante à grand volume de la diffusion par la glace de lac se traduit par une détérioration de la cohérence du lac, qui contraste bien avec la cohérence plus élevée de la terre autour, et qui peut souvent être facilement distinguée de celle-ci.

Le besoin même d'une fenêtre de pixels d'échantillonnage pour évaluer la cohérence limite, et réduit réellement, la résolution de la carte de cohérence par rapport à la résolution inhérente de l'image de rétrodiffusion radar. On peut régler ce problème en modifiant la taille et la forme de la fenêtre d'estimation, en utilisant des cartes de cohérence multi-résolution, en

ajoutant à la carte de cohérence l'image de rétrodiffusion radar à résolution plus élevée qui peut facilement être obtenue, des images de phase d'interférogramme ou des images résiduelles, ou en adoptant une approche multi-temporelle.

Mattar, K., Buchheit, M., Beaudoin, A., 2001, Shoreline Mapping Using Interferometric SAR, DREO TR 2001-078, Centre de recherches pour la défense Ottawa

This page intentionally left blank.

Table of contents

This page intentionally left blank.

List of figures

List of tables

Acknowledgements

This study is a result of a collaboration agreement between SPOT Image and DREO. SPOT Image provided the InSAR pairs over McKenzie Delta and the Bay of Fundy. These were both processed by Gamma Remote Sensing AG, Switzerland. The pairs over Duck and Onslow beach were processed by Atlantis Scientific Inc., Ottawa, Canada. The Bathurst Island pair were processed at CCRS. The ERS data is copyright ESA.

Introduction

Interferometry is one of the most significant tools to have evolved from Synthetic Aperture Radar (SAR) in recent years. Single and repeat-pass Interferometric SAR (InSAR) have both been used for topographic mapping, as in the recent Shuttle Radar Topographic Mission (SRTM). Repeat-pass across-track InSAR has also been used for displacement measurement and classification studies in such wide-ranging applications as crustal dynamics, glaciology and classification of vegetation and terrain [7]. Above all, InSAR is now playing a major role in building global topographic databases.

Shoreline mapping using space-borne SAR, and specifically Satellite Radar Interferometry (SRI), has received renewed attention recently from a variety of sources. As well, the related problem of automatic water-body masking is of great importance to the successful generation and refinement of topographic maps from SRI or InSAR (such as those from the SRTM). NIMA (the US National Imagery and Mapping Agency), for one, has undertaken to significantly improve its hydrographic coastal databases and hopes to benefit from these techniques by increased accuracy, reduced costs and more rapid completion. Both are also needed for such diverse applications as flood monitoring, maritime operations and shipping, and logistical support for marine landing forces.

Given the increasing importance and role of these two problem domains, and of RSI topographical mapping in general, the main focus of this study is to explore various repeat-pass InSAR tools, coherence being one of the more significant ones, for delineation of shoreline and lake boundaries. Since shoreline environments vary greatly, an integral part of this study is the examination of the coastal geomorphology and vegetation that may aid or limit the accuracy of such tools.

In the first section, we outline the significant InSAR processing steps and considerations necessary for calculation of the interferogram and accurate estimation of the coherence. In the second section, we examine the various factors (both desirable and adverse) that can contribute to decorrelation of the interferometric pair. In the third and last section, we examine the problem of shoreline mapping in particular, and explore various InSAR tools that can be used in this application, using five coastal areas as examples: four in regions with temperate environment and one in the Arctic environment. The four temperate locations consists of Duck Beach (North Carolina, USA), Onslow Beach (near Camp Lejeune, North Carolina, USA), MacKenzie Delta (NWT, Canada), and the Bay of Fundy (Nova Scotia, Canada). The single Arctic scene is of the eastern portions of Bathurst Island (Nunavut, Canada).

Estimation of coherence

The calculations of the interferogram and coherence map from the interferometric pair are outlined in Figure 1. The processing begins with a pair of single look complex (SLC) images, usually referred to as the master and slave images. Range and azimuth spectral filtering serves to increase the image coherence, at the expense of resolution. Azimuth spectral filtering also serves to reduce baseline decorrelation (see next section). The larger the baseline between the interferometric pairs (up to the critical baseline), the greater the improvement the azimuth spectral filtering has on the coherence. For applications like shoreline mapping where resolution is critical, this step could be limited in scope or avoided altogether. Fine registration of the slave to the master is a standard procedure for interferometry. Accurate fine registration is important and can have a significant effect on coherence, especially for SAR systems such as RADARSAT that operate with an azimuth squint angle [9]. Normally the flat-earth phase component is removed from the slave image before calculation of the interferogram. Removal of both the flat-earth phase component and, in the case of mountainous terrain, the topographic phase component are critical step in the coherence calculation. Finally, the coherence map can be resampled to a lower resolution by averaging or decimation.

The coherence is a measure of the degree of correlation between two complex data sets. The interferometric coherence magnitude, δ, can be estimated by a sample statistic given by [10]:

$$\delta = \frac{\left| \sum_{i=1}^{L} z_{1i} z_{2i}^{*} \right|}{\sqrt{\sum_{i=1}^{L} |z_{1i}|^2} \sqrt{\sum_{i=1}^{L} |z_{2i}|^2}}, \qquad (1)$$

where i is the sample number, L is the number of samples in the coherence window, and z_1 and z_2 are the single look complex (SLC) image of the master and slave. The size of the coherence window, and hence the number of samples used in the coherence window, is an important consideration. There are significant advantages and disadvantages to choosing both small and large coherence windows. Clearly, there is a trade-off between resolution and usefulness of the estimated coherence. Smaller windows yield better resolution, but will produce a more biased coherence estimate, generally exhibiting a lower contrast between the high and low coherent portions of a scene [10]. On the other hand, large windows resolve the latter two issues at the expense of resolution. For shoreline mapping where the **location** of the interface between the high and low coherent areas is critical, one would like both a small window for optimal coherence resolution and large window for maximizing the difference between high and low coherent portions of the scene. A compromise can be achieved in two ways. First, by choosing an optimal window size and shape. If this approach is unsatisfactory and higher resolution is needed, a multi-resolution coherence approach can be used. A low resolution, high contrast, coherence map is used initially to roughly define the shoreline, followed by a higher resolution, lower contract, coherence map to identify it more precisely.

Alternatively, the coherence map can be supplemented with the full resolution amplitude and/or phase image. For the tests in this study the first of these approaches is used.

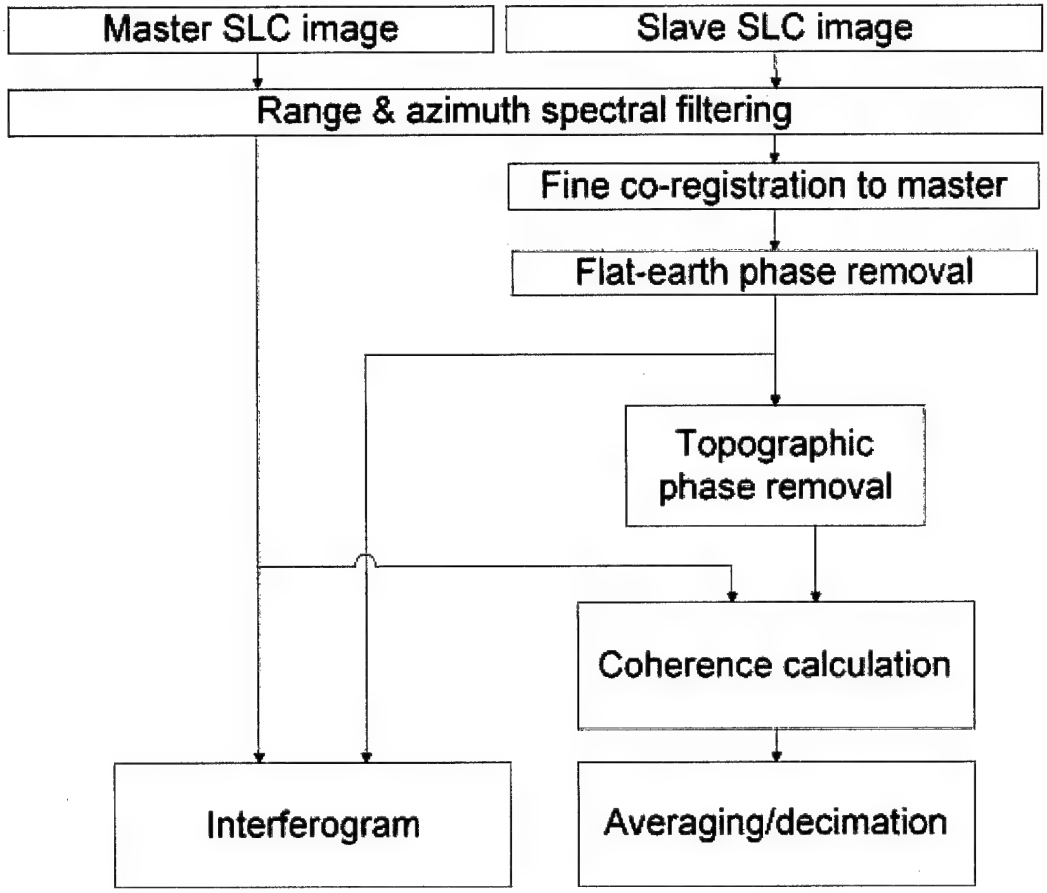

Figure 1: *Flow chart for interferogram and coherence derivation using the single look complex (SLC) master and slave images as inputs.*

Decorrelation in Interferometric SAR

Coherence has become an important tool within repeat-pass SRI. It is also a key limitation to the dependability of SRI applications. There are many factors that can cause degradation in the scene coherence. Consequently, at best, these limit the resolution and usefulness of SRI applications and, at worst, completely block them. It is useful to list some of these decorrelation factors and examine means of overcoming, or at least reducing them, where possible. The total observed correlation δ_{total}, or decorrelation $(1-\delta_{total})$ can be given in terms of the product of some of the more significant correlation factors:

$$\delta_{total} = \delta_{thermal} \times \delta_{temporal} \times \delta_{baseline} \times \delta_{troposphere} \times \delta_{ionosphere} \times \delta_{coregistration} \times \delta_{volume}. \quad (2)$$

Let us consider each of these correlation factors separately:

Thermal: $\delta_{thermal}$ is the thermal correlation coefficient and is a function of the thermal noise of the two systems. It can be given by [11]:

$$\delta_{thermal} = 1/(1+SNR^{-1}), \quad (3)$$

where SNR is the signal-to-noise ratio of the system. Obviously for any given system, this value normally does not vary.

Temporal: $\delta_{temporal}$ is the temporal correlation coefficient. It is one of the more detrimental factors in SRI. It would include, for example, any changes in moisture of the terrain due to precipitation, and random movement of the prime reflective components of vegetation or forest cover. Many (but not all) of these factors are highly dependent on the wavelength of the system. For example, at X-band, the main scatter from a tree may be due to the small branches and leaves. At larger wavelengths such as L-band, the main scatter of the tree may be from the main trunk, which is less susceptible to movement. Therefore depending on the circumstances, the temporal decorrelation coefficient may be reduced by using a longer wavelength radar (e.g. L- or P-band), by reducing the time interval between acquisitions of the interferometric pair, or by repeated trials hoping that one pair will have a sufficiently low decorrelation.

Baseline: $\delta_{baseline}$ is the baseline correlation coefficient. It is a maximum when the two antennae that make up the InSAR pair view the ground scatterer from the same viewing angles (though not necessary from the same distance). This occurs when the component of the baseline perpendicular to the range direction of the master satellite (called the perpendicular baseline) is zero. As the perpendicular baseline increases, the ground reflectivity spectra acquired by the two antennae becomes increasingly divergent, the scene coherence is reduced, and the baseline correlation coefficient decreases. Beyond a certain critical value (called the critical baseline), coherence between the pair is completely lost. The critical baseline, $B_{\perp, cr}$, is given by [3]:

$$B_{\perp, cr} = \lambda R \tan\theta / 2R_r, \quad (4)$$

Where R_r is the slant range resolution, λ is the wavelength, R is the slant range, and θ is the nominal incidence angle. For ERS-1/2, for example, this critical baseline is ~1100 meters.

When the perpendicular baseline lies between these two extremes, filtering can be used to select the common portions of the reflectivity spectra. This will increase the scene coherence, but only at the expense of resolution.

Troposphere: Tropospheric decorrelation, $(1-\delta_{troposphere})$ is among the more difficult decorrelation factors to reduce, let alone predict. In some cases it is observed as a ghost-like figure in the coherence map. In other cases, as with atmospheric gravity waves, a distinctive pattern can be observed in the interferogram phase, and once detected can be reduced by an appropriately designed filter. In most cases, the tropospheric effects on any given interferogram are subtler but by no means less significant [6]. If a reference digital elevation model (DEM) is available, the difference in slant range between the measured interferogram phase and the topographic phase (as calculated from the DEM) may reveal the existence and magnitude of any tropospheric effects. The user may then be able to judge the significance of the effect and, if serious, can either find a better pair or attempt to improve the existing one by filtering. In practice, tropospheric problems often remain unnoticed, with consequent degradation to the accuracy of the final results.

Ionosphere: Ionospheric decorrelation $(1-\delta_{ionosphere})$ is less serious than the tropospheric decorrelation. Its distinctive linear "streaking" pattern is often clearly visible in the coherence map. The magnitude of the effect can be estimated by calculating a map of the azimuth shift needed for optimal coherence. In DEM generation applications, the azimuth shift can also be used in a first order correction of the interferogram phase.

Co-registration: $\delta_{co\text{-}registration}$ refers to the coherence factor due to linear and circular co-registration errors between the master and slave images. This can be an important factor in SARs operating with a squint. For example, for a RADARSAT system operating in stripmap mode with a yaw angle of 3 degrees, an interferometric phase error of about 30 degrees occurs from near to far range if the interferometric pair is misregistered by 0.1 sample in azimuth [9].

Volume: Finally, $(1-\delta_{volume})$ is the volume decorrelation factor. This would include decorrelation due to multi-path scattering, from scattering from two or more differing surfaces within a volume, such as the leaves and trunk of trees in a forest, or the from the air/ice interface and interface between differing ice layers within a glacier in the Antarctic.

This is, by no means, an exhaustive list of decorrelation factors. Not included in the above list, for example, is decorrelation due to systematic processing errors.

Shoreline Mapping and Water Body Masking

The successful use of any interferometric SAR methodology for shoreline mapping and water body masking is highly dependent on the geomorphology and vegetation of the coastal region, as well as the stability of the shoreline itself. The very definition of a shoreline is application dependent. For updating the hydrographic coastal databases, NIMA defines the shoreline by the *Mean High Water Level* (MHWL). In other applications, the low tide water level may be more significant. More problematic are very shallow regions that are exposed to very large tidal variations. In certain locations of the Bay of Fundy, for example, not only does the location of the shoreline vary greatly depending on the tides, but small islands and shorelines disappear altogether at high tides.

Radar is sensitive to the geomorphology of the terrain. The radar backscatter will vary according to the type of scatterer on the coast; sand, gravel, pebble, bedrock or vegetation are a few examples. The backscatter from vegetation will vary according to its density, height, type, moisture content, etc. The structure of the reflecting surface is also obviously very significant. However, for these applications the radar backscatter is perhaps most sensitive to the water content of the terrain. The largest variation in the radar backscatter may, for example, not be between the water and coast, but between a water-drenched sandy beach and the vegetation or bedrock behind it. Certain topography can obscure the shoreline altogether. A cliff or other sudden and dramatic change in the terrain elevation near the beach can completely obscure the coastline because of radar layover or shadow. In Figure 3(b) for example, the bright line in magnitude on the east side of Blomidon Peninsula is due to layover and should not be confused with a shoreline. If imaged from the opposite direction, the shoreline would likely fall within the radar shadow.

The radar captures a brief snapshot in the dynamics of the shoreline. The location of the shoreline will not only change with tidal variations, but more subtly with the phase of the waves. This becomes highly significant in high resolution mapping applications.

Interferometric SAR makes use of the correlation (or the lack of it) between two passes of the radar that are nearly identical geometrically (though not necessarily temporally). Shifting sands, growth of the vegetation, movement of the trees, changes in the surface moisture of the terrain or vegetation between passes will all have an effect on the correlation of the interferometric pairs and, therefore, also on any information extracted from them.

It is useful to consider and study shoreline mapping in temperate environments separately from shoreline mapping in Arctic environments. In temperate environments, the shoreline is ideally defined by the interface between the absence of coherence on the oceans or seas, and the relatively much higher coherence of the land. By contrast, in an arctic climate, both the frozen seas and (frozen) land usually have relatively high coherence. The coastline is defined by a ribbon of low coherence that is formed between the near shore land and the near shore sea ice that is constantly being subjected to tidal variations or differential melting. ERS-1/2 SRI data were collected over four regions in temperate climate and over Bathurst Island in the Canadian arctic. Details of these passes are listed in table 1. Using this data, let us consider each of these categories in more detail.

Table 1: *List of ERS-1/2 SRI data used in this shoreline mapping study*

Name of site	Scene latitude (degrees)	Scene longitude (degrees)	Date	Pass Orientation	Perpendicular Baseline (m)
Bay of Fundy, NS, Canada	N45.377	W64.540	5/6 Apr '96	Desc.	-68
Mackenzie Delta, NWT, Canada	N64.053	W135.48	25/26 Apr '96	Desc.	-79
Duck Beach, NC, USA	N35.7	W75.8	5/6 Oct '99	Desc.	-275
Onslow Beach, NC, USA	N34.436	W77.521	8/9 Oct '99	Desc.	-269
Bathurst Island, NU, Canada	N75.16	W97.14	7/8 Feb '96	Asc.	187

Temperate Environments

The problem of finding suitable methodologies for coastal shoreline detection and extraction using SAR data in general can benefit from careful use and interpretation of the interferometric coherence between successive SAR passes, augmented by their backscatter magnitude images. In temperate regions where no ice or frozen areas exist, the assumption commonly made is that open sea will decorrelate rapidly while land (and particularly, urban) areas will remain relatively unchanged (high correlation) over the time elapsed between the first and last pass. The hope is that ERS 1/2 tandem data (with a one day time separation) will exhibit these ideal properties.

The discussion and results presented here are part of a larger study on the above problem. That study was not restricted to ERS 1/2 tandem data, but also considered multi-pass, multi-date SAR SLC scenes from both ERS and RADARSAT-I. Several approaches were investigated to augment and extend the use of the interferometric coherence by combining it with temporally and/or spatially filtered backscatter imagery gathered over more than two dates. This approach is beneficial in various ways: reduction of speckle, enhancement of changes, and above all, extension of the data sample space allowing better discrimination of the land/sea (or land/water) interface by classification and segmentation methods.

The concept of coherence can also be extended from the interferometric one used in Equation 1. In the case of single pass filtered backscatter imagery, texture classification can be used, where the texture measure is defined by the spatial coherence within a scene (i.e. the 2-D cross-correlation of neighbouring regions). In the multi-pass, multi-temporal case, coherence can be extended to a multi-dimensional cross-correlation or, alternatively, a set of

interferometric (or temporal) coherence measures over various time periods (one day, one month, one year).

The Scenes under Study

Four regions in temperate environments and one arctic area during spring thaw (the Mackenzie Delta, NWT) have been studied as part of the larger study previously discussed. Each scene is characteristically different and illustrates the difficulties of the shoreline extraction problem under diverse conditions (see Table 1 for scene parameters).

Various factors and parameters come into play in the problem of coastal shoreline detection and mapping that not only affect the detected backscatter amplitude of each single pass, but also have profound effects on the interferometric coherence of each pair. These are:

1. Inherent sensor related factors:
   - Polarisation: VV (as in ERS) is not as effective as HH in creating good land/sea radar contrast.
   - Incidence and azimuth viewing.
   - Resolution limitations (ERS 30m).
2. The near-shore ocean surface turbulence:
   - Wave spectrum (wave energy, height and direction).
   - Tidal stage.
   - Breaker characteristics.
3. Coastal geomorphology and topography:
   - Beach material constituents (sand, gravel, pebble, bedrock, etc).
   - Dunes, cliffs or shallow flood plains.
   - Near and back-shore soil types (moisture retention characteristics).
4. Coastal and back-shore vegetation:
   - Types and densities (scattering characteristics).
5. Meteorological conditions and changes:
   - Wind velocity affects the scattering from certain vegetation classes and from dune or sandy regions, and consequently will affect (interferometric/temporal) coherence.
   - Precipitation affects scattering from vegetation and soil depending upon their moisture retention characteristics, and consequently changes in the precipitation between an InSAR pair will affect the coherence.

All of these factors affect the efficacy and robustness of any automated method to derive and extract coastal shoreline.

Scene Processing

Each of the scenes was interferometrically processed as in Fig. 1. None of the scenes was corrected for topography. Further, post processing was done to create so-called "*ILU*" (*Interferometric Land Use*) false colour composites that are useful as tools for scene quality assessment, interpretation and change detection. It was also an objective to study the efficacy of the ILU representations in the automatic classification and detection of coastal shorelines, therefore two types of ILU composites were used:

- ESRIN "*CAR*" type ILU product: Coherence (δ) is represented as the "red" channel, the average of the backscatter magnitude (σ_0) for the pair as the "green" channel, and the ratio of the slave to master σ_0 as the "blue" channel.
- ESRIN "*CFA*" type ILU product: Coherence (δ) is represented as the "red" channel while the two channels as "green" and "blue".

The Blomidon Peninsula

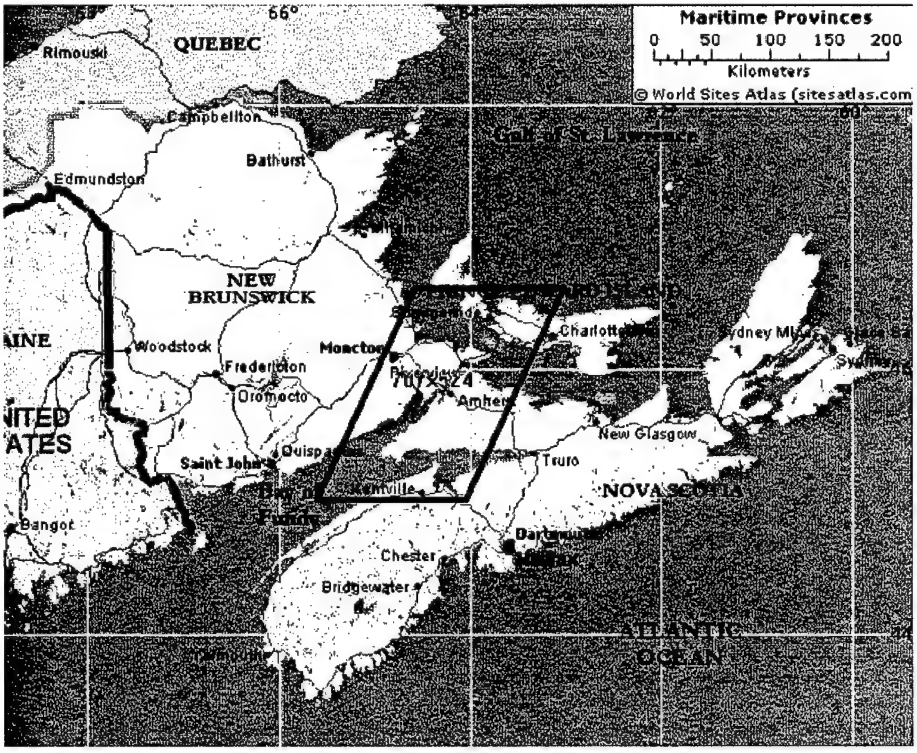

Figure 2: *Map showing the Bay of Fundy test site*

Generally, those regions in the scenes appearing bright in "red" have a high coherence level, while those appearing yellow or white are areas of little change. So called "permanent point scatterers" (most man made structures and some types of geological structures) would appear as bright white points. Areas of low coherence would be shades of blue, cyan or green. In the case of a SAR image, large changes will be mostly blue.

Figure 3(a) and (b) show the Blomidon Peninsula located in the Bay of Fundy, Nova Scotia (see map in Figure 2). This is a region exhibiting extreme topology (very steep cliffs by the ocean) and extreme ocean surface turbulence (very large and rapidly changing tidal levels — some of the largest on the continent). Contrast this with the opposite extreme of the Mackenzie Delta (see next section).

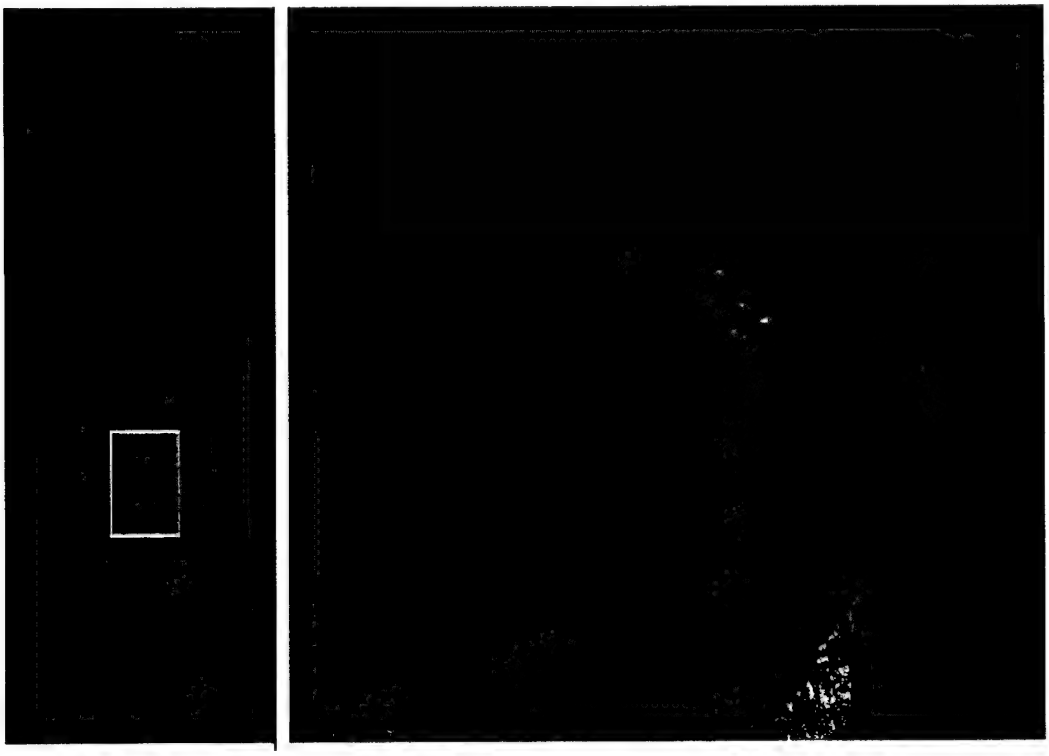

Figure 3: *(a) ERS tandem pair shown as an ESRIN "CFA" type ILU product of the Bay of Fundy, Nova Scotia and (b) the region of interest - the Blomidon Peninsula (acquired April 5/6, 1996.)*

The very steep topology of the Blomidon Peninsula can lead to strong radar layover when viewed from one side, and radar shadow when viewed from the other side. Obtaining ground control becames difficult. Effects of the beach geo-morphology are also clearly visible. The beach on the eastern side consisted of large rocks/pebbles having good scattering properties, but was completely obscured in the radar image by the layover of the cliff near the shore. On the other hand, the beach on the western side was comprised of smooth sand with different imaging characteristics.

The overall scene is highly incoherent, probably not only due to the tremendous ocean surface turbulence changes (green/blue) but also due to the meteorological conditions and the vegetation (trees/forests) cover at the time. By contrast, some of the man-made structures, the urban areas, and farmed fields are clearly outlined by the coherence and are visible in the figure as red or white.

One may conclude from studying this scene and those similar to it, that visual interpretation of such scenes using only a single tandem InSAR pair remains very difficult. Classification or

detection of shorelines in this situation will have large ambiguities due to an overall lack of coherence and the scattering phenomenology. Knowledge of the near shoreline constituents, the weather and the ocean surface turbulence is necessary for successful interpretation and shoreline classification.

The Mackenzie Delta

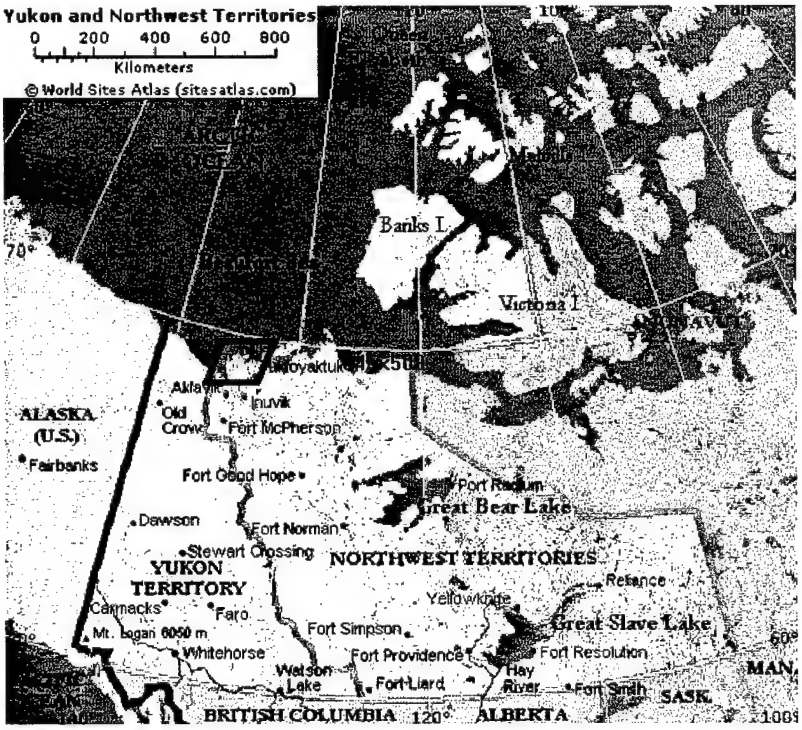

Figure 4: *Map showing the Mackenzie Delta test site*

Figure 5(a) and (b) show a small portion of the Mackenzie River delta, in the Northwest Territories, Canada during the spring (see map in Figure 4). This is also an area of extreme topology (flood plains; very flat and highly variable). The so-called "shoreline" (land/ice/water interface) boundary variations here are small in elevation, but are extremely far ranging and random horizontally due to the extremely low relief. Tides cause very large excursions of the waterline ranging over tens of kilometres in a relatively short time span.

High coherence may be seen over bare land or frozen land-cover (relatively stable over short time periods), while the rapidly changing nature of the estuary in spring is clearly visible in contrast (low coherence, high changes in backscatter).

Since the estuary area has tides and "water lines" that are so highly variable, these can only be defined in "fuzzy" or probabilistic terms. Boundaries (land/ice/sea) can be extracted with adequate precision automatically, but are rendered meaningless or unreliable in the long term because of their high variability. Compounded by very little ground truth and a dearth of

reliable topographical maps for the area, "shoreline" extraction accuracy is expected to be very low compared to existing data.

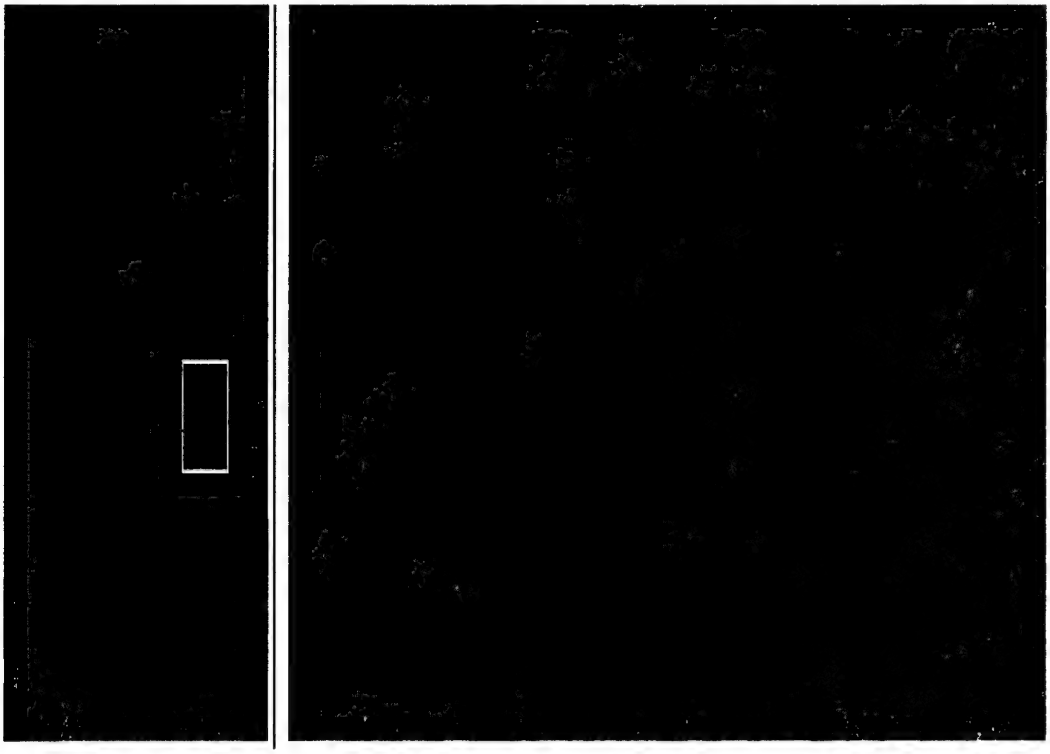

Figure 5: *(a) ERS tandem pair shown as an ESRIN "CFA" type ILU product of the Mackenzie Delta and (b) the region of interest (acquired April 25/26, 1996.)*

North Carolina Shoreline: Duck Beach and Onslow Beach

These two areas on the North Carolina shoreline (see map in Figure 6) were a part of a larger joint DREO/NIMA shoreline mapping study. The region has a highly variable shoreline and shore/vegetation interface. Acquisition dates were just a few weeks after Hurricane Floyd hit the area, adding to the phenomenological complexity of the data (and also made it interesting for change detection purposes). Both scenes exhibited large breakers (affecting the use of backscatter). Low tidal ranges (tidal stages ranged from 1m to 10-15m horizontal shift) were not an issue.

The areas have been heavily surveyed by USGS and NIMA. Therefore, high resolution ground truth is available in the form of 1m ortho-quads, GPS and high resolution LIDAR (30 cm footprint) coverage. In addition, a vast amount of very accurate and highly sampled tidal and sea/state data was obtained, as well as records of the local near-shore geomorphology and topology. Let us examine these two areas in more detail.

Duck Beach, Currituck Sound, N.C.

Figure 7 (a) and (b) show the Duck Beach area near Currituck Sound, North Carolina. The shoreline region can be characterized by a highly variable boundary between sandy beach and vegetation, a smooth to rough sand transition above the high tide marks, and some developments close to the beach.

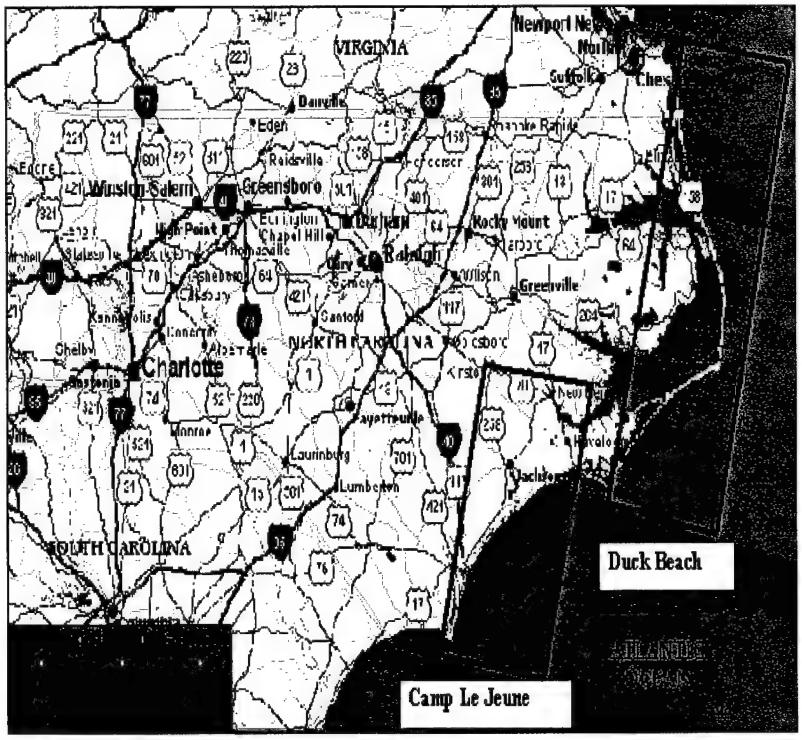

Figure 6: *Map showing the North Carolina test sites*

High coherence areas are only visible in the back-shore terrain, in developed land or from man-made structures. The coherence near or at the shoreline is very poor in general. This may be due to a variety of phenomena at play: vegetation types, soil and sand characteristics and the weather effects on these. Detailed study of the scene has shown that overall shoreline edge contrast is patchy and unreliable. For this scene, use of the backscatter channels as a complementary aid is also hindered for the same reasons and there is also little differentiation in clutter statistics over the open water and the near-shore regions (where coherence is poor).

Onslow Beach, New River area, N.C.

Figure 8 (a) and (b) show the Onslow Beach area near New River, N.C (see map in Figure 6). Again, in the near-shore regions, the observations and conclusions are similar to those discussed for Duck beach above. However, the general area is much more stable because of the large degree of land use and development, both inland and near-shore (manifested by the

high overall coherence). In the undeveloped shoreline area, deep sandy beaches and large sandbanks in inlets contribute to further problems.

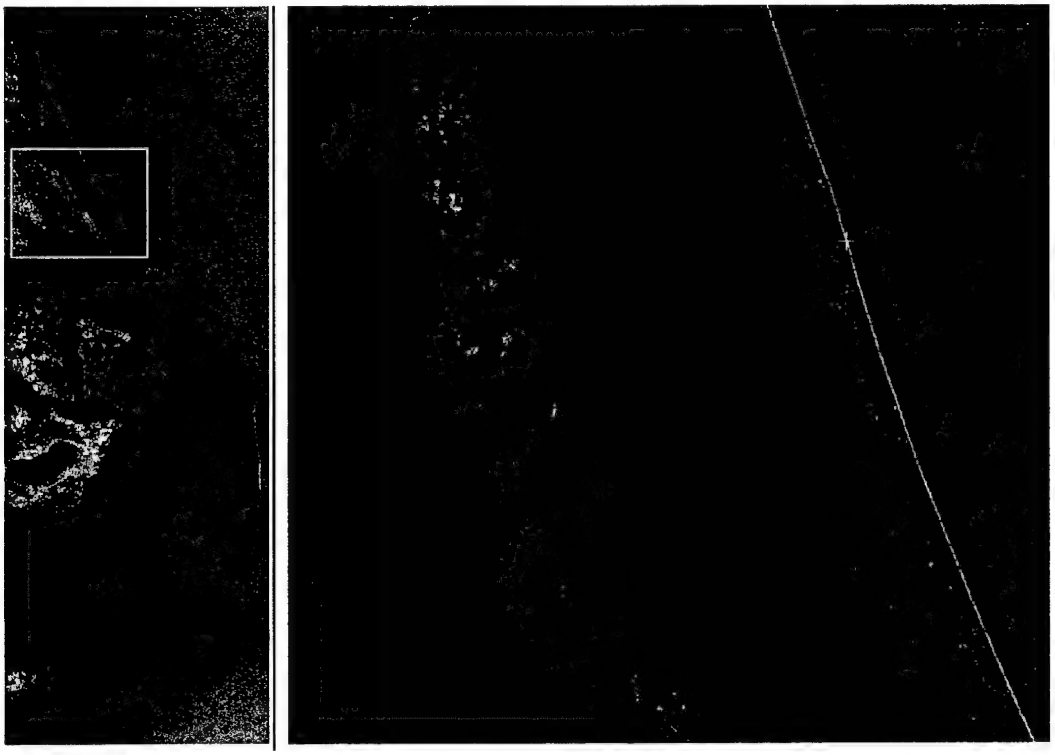

Figure 7: *(a) Northern half of an ERS tandem scene over Currituck Sound, N.C. and (b) the region of interest, Duck Beach (insert). Representation is a CFA type ILU product. The scene on the right has been geocoded and overlaid with a USGS MHWL shoreline vector (in yellow).*

Both scenes characterized the problems of shoreline mapping for highly unstable sandy beaches with shallow tidal stages. In both, the detected shoreline boundary departs significantly from the true MHWL. In the Onslow Beach case, detected shoreline accuracy of 30m using ERS data may be achievable under ideal circumstances. The same cannot be said for Duck Beach.

Summary

In temperate environments, there are a number of inherent problems with the use of interferometric coherence, either alone, or in conjunction with the pair's backscatter amplitudes, for deriving accurate shoreline maps. These can be summarised as follows:

1. The coherence is too variable in back-shore land/vegetation and too subject to meteorological conditions and moisture retention. Classification techniques or thresholding methods fail at the shoreline (no problem with urban or permanent structures, or bare rock formations).

2. The use of a single pair contributes only two dates of observations. Multi-temporal and multi-pass datasets would extend the temporal component of the data.

3. Thresholding classifier techniques in a high clutter, high noise regime will fail with high misclassification results. Statistical (or textural) classification techniques (in the single dataset case) fail because backscatter and clutter statistics over land and sea are too similar (poor backscatter contrast and differentiation) due to weather, ocean surface turbulence, and geomorphology.

4. Coastal geomorphology varies from region to region. Shore types with larger beach material size show better contrast and are therefore easier to detect. However, a technique that works successfully in one type of region may not be applicable at all in another region (e.g. North Carolina versus Mackenzie Delta).

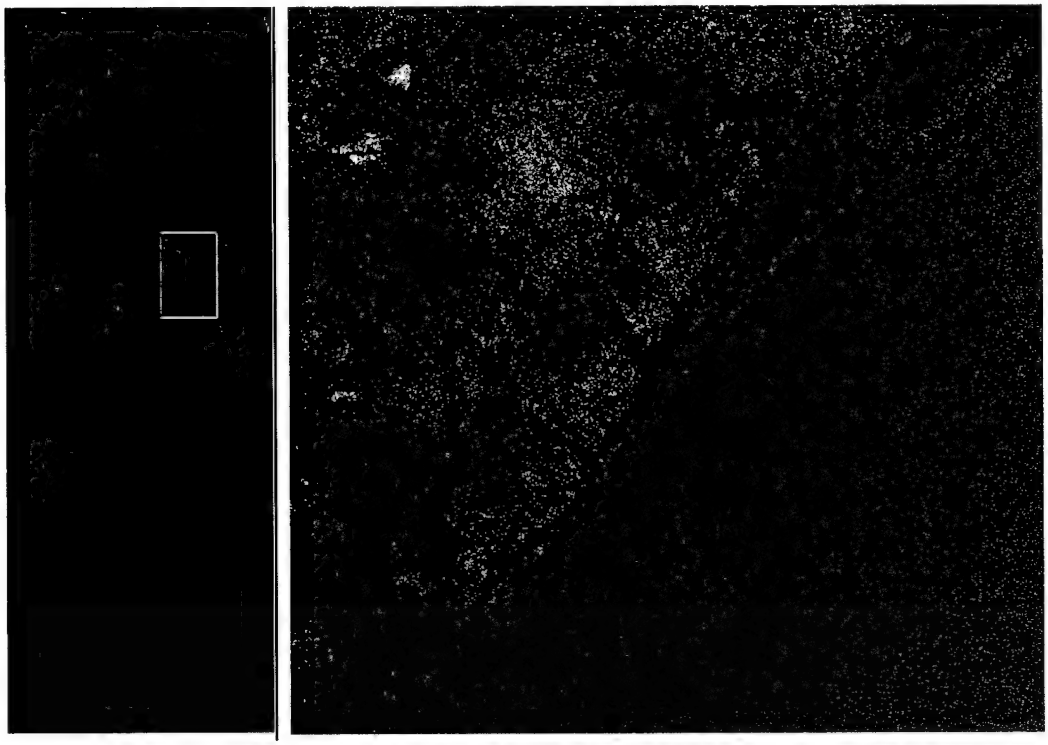

Figure 8: *(a) ERS tandem scene over New River, N.C. and (b) the region of interest, Onslow Beach, Onslow Beach. Representation is a CFA type ILU product.*

In addition there are a number of data processing issues that can further limit accuracy:

1. Ortho-rectification and geo-coding accuracy. These are limited by the accuracy of the software methods used (and may be beyond the user's control) and its ability to utilise accurate orbital data. In some cases, further ground control point (GCP) acquisition must be done through the use of independent ground truth sources and GPS. These issues limit whether the accuracy of the geocoded data is at its ideal optimum or not (approximately 30m for ERS data).

2. Coherence estimation accuracy trades off against resolution.

3. Co-registration errors. In the single pair case, this is subject to the inherent accuracy of the software methods used. If multiple datasets are used, then additional sources of coregistration error will be incurred.

A number of approaches can be used to mitigate these limitations:

1. Make use of multi-temporal and multi-pass datasets to extend the dataset. This will help to minimise classification errors by providing more information to differentiate the signature of each "class", while also suppressing the relative levels of noise and clutter. It will also afford opportunities for data fusion, through temporal and/or spatial filtering, and exploitation of principal components to de-couple (de-correlate) independent datasets. This benefits not only classification, but also change detection and interpretation.

2. Allow more processing control over the coherence estimation (interferometric or other), so that it can adapt to the inherent variability within a scene.

3. Extend the concepts of coherence and of texture mapping to form multiple datasets and multi-temporal data. Both types of measure are related and may be promising over larger time durations. The spatial-resolution/accuracy trade-off (see above) will be improved by the increased information content.

Arctic Environments

Unlike temperate climate regions, in arctic climate environments, both the sea and the land often maintain a relatively high coherence over an extended period of time. The tides subject the frozen seas to constant vertical displacement. Most often, the interferometric pair captures the sea ice in two different phases of the tidal cycle. As a result, a thin shear region of low coherence results between the displaced frozen sea and the fixed land. It is this thin zone of low coherence that we hope to take advantage of to detect and define the shoreline.

Bathurst Island in Nunavut, in the Canadian arctic (see Figure 9) was used as the test site. The island has the advantage of being rocky, barren, with relatively low relief - ideal conditions for SRI. The ERS-1/2 tandem passes were acquired on 7/8 February 1996 (ascending orbits), and have a perpendicular baseline of approximately 187 meters. Processing of the data follows the outline in Figure 1, but with no topographic phase correction. The amplitude of the master, the interferogram phase, and the coherence map are shown in Figure 10 (from left to right). A coherence window of 15 lines in azimuth by 3 pixels in range was used. The shoreline is clearly outlined in the coherence map, but not always in the amplitude image. This is more clearly visible in the enlargement of inset 'A', shown in Figure 11. In portions of the amplitude image in the centre of the scene, the shoreline is, in fact, ambiguous. The very same shoreline is clearly defined in the coherence image. This is even more clearly demonstrated in Figure 12, which shows a plot of 3 lines along the cut drawn in the first image of Figure 10.

This case clearly shows the advantage of using the coherence over amplitude for shoreline mapping. Combining both the coherence and amplitude images will improve, simplify and refine the coastline mapping procedure. For circumstances requiring a higher resolution than that available using a coherence map, one could utilize the full resolution amplitude image to refine a coherence based shoreline extraction procedure. The amplitude image may also help distinguish cracks in the ice (visible in the coherence image) from the coastline. These cracks are shear zones between different ice plates, each moving slightly differently under the general influence of the tidal cycles.

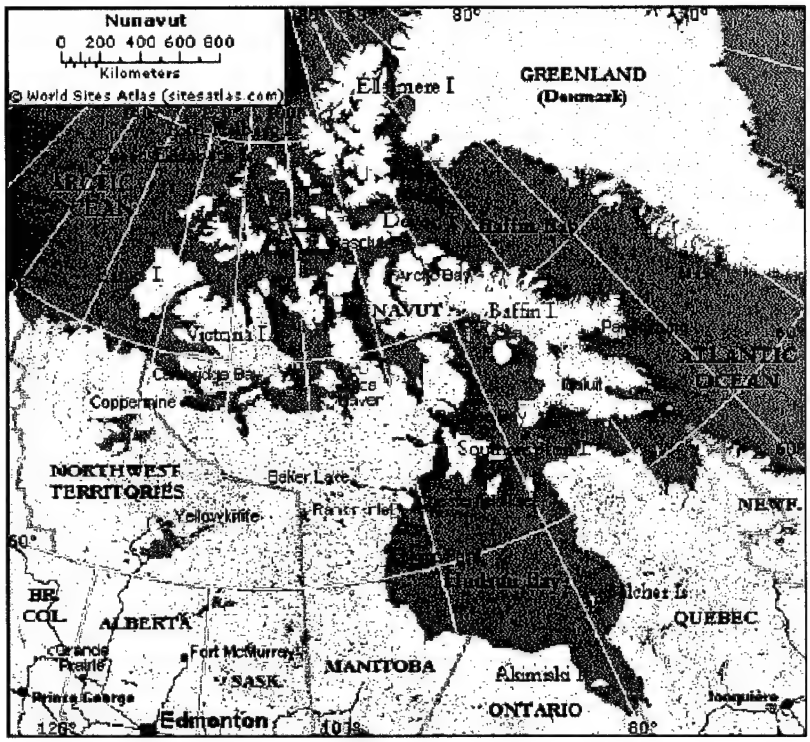

Figure 9: *Map showing the Bathurst Island test site*

Lake masking is another significant application where the coherence map can prove useful. Lake Ice is filled with air bubbles, as well as perhaps cracks and debris. All of these contribute to the radar backscatter, leading to a volumetric scattering mechanism. In contrast with the surface scattering mechanism of the surrounding land, the lake will consequently exhibit an apparently higher phase noise. This sudden change in the phase noise will be readily visible as a change in coherence, as is demonstrated in Figure 13. Figure 13 shows an enlargement of inset 'B' shown in Figure 11. Clockwise from the top left is the amplitude of the master, the coherence map, the lake mask resulting from applying a threshold and filter to the coherence map, and the interferogram phase. The lakes, barely distinguishable in the amplitude image even by eye, are clearly visible in the coherence map.

For DEM generation applications, if these areas (in addition to the shoreline) are not masked out, they will lead to a false elevation model. The use of such coherence images could form the basis for a useful tool for automated (or semi-automated) lake masking.

Figure 10: *Amplitude of master (left), interferogram phase (centre), and coherence (right) of Bathurst Island ERS-1/2 tandem data, acquired 7/8 February 1996. Near swath is along the left of the scene. The scene measures approximately 44.4 km in azimuth by 26.5 km in slant range (approximately 67.2 km in ground range). A 15 x 3 (azimuth x range) pixel window was used in the coherence calculation. 3 x 3 averaging was in the calculation of all three images.*

Figure 11: *From left, the amplitude of master, interferogram phase, coherence, circular variance and residue of Bathurst Island ERS-1/2 tandem data, acquired 7/8 February 1996. Near swath is along the left of the scene. The scene measures approximately 19.0 km in azimuth by 4.0 km in slant range (approximately 10 km in ground range). 3 x 3 averaging was used in the calculation of the first four images, and the coherence image used as input to the circurlar variance calculaiton.*

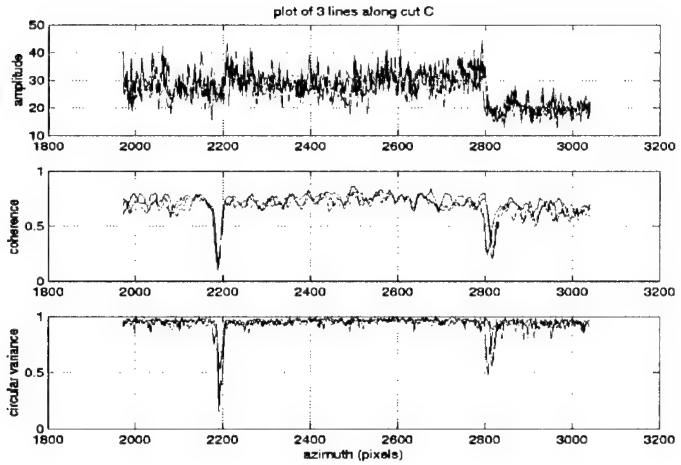

Figure 12: *Plot of 3 individual lines along the cut shown in the first image of Figure 11. From the top are the amplitude of the master, coherence, and circular variance.*

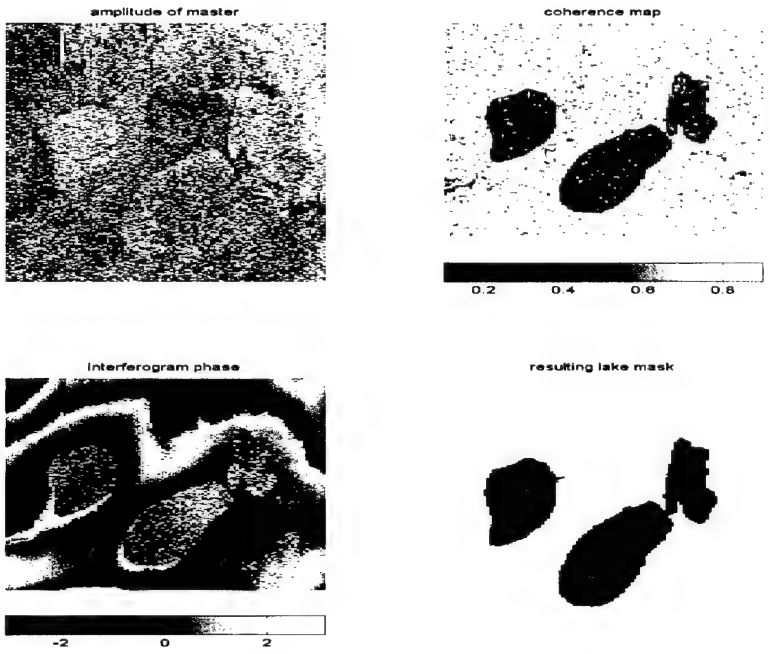

Figure 13: *Subscene 'B' from Bathurst Island scene of Figure 10. Clockwise from the top left is the amplitude of the master, coherence, lake mask resulting from applying a threshold and filter to the coherence map, and interferogram phase.*

Alternate InSAR Tools

Coherence is essentially a measure of the phase noise in an interferogram. Other tools are available that provide a similar measure, and may have advantages over the coherence. The most significant of these are the circular variance and the residue. The circular variance can be defined as [5]:

$$V = \sqrt{\bar{c}^{-2} + \bar{s}^{-2}}, \tag{5}$$

where $\bar{c}$ and $\bar{s}$ are the local averages of the sine and cosine of the interferogram phase angle. Clearly V decreases from 1, for no phase variation within a given window of pixels, towards 0 as phase noise increases. Similar to the coherence map, the resulting resolution of the circular variance map is reduced since it needs to be calculated over a window. The shape of the window can, once again, be varied, or a multi-resolution window approach used in order to improve resolution. It has one important advantage over the coherence. Whereas the coherence requires the full resolution, single look complex master and slave images at input (which may take up a lot of physical memory), the circular variance requires only the interferogram phase, either in full resolution or smoothed. The circular variance for subscene 'A' of the Bathurst Island scene is shown in the fourth image panel from the left of Figure 10, and in the plot of bottom plot of Figure 12. The coherence (shown in the third panel of Figure 10) served as input to the circular variance calculation. The circular variance was calculated over a 3x3 window. This map compares favourably with the coherence. In some applications the coherence map may have more benefits, in others the circular variance.

The residue field detects the presence of discontinuities in the interferogram phase. It is another tool that has found a critical application in phase unwrapping and could be useful at times in extracting information from an interferogram, by supplementing the coherence, circular variance or magnitude maps. Like the circular variance, the residue works directly on the wrapped phase, ψ (or unwrapped phase, ϕ), either in full resolution or filtered format. It is defined as [4]:

$$r(i+½,k+½) = W\{\Delta_i\psi(i,k)\}+W\{\Delta_k\psi(i+1,k)\}-W\{\Delta_i\psi(i,k+1)\}-W\{\Delta_k\psi(i,k)\}, \tag{6}$$

where:

$$\psi = W\{\phi\} = \mathrm{mod}\{\phi+\pi,2\pi\} - \pi, \tag{7}$$

and where Δ_n is the difference operator in the direction defined by 'n'. The residue has a value of either zero (no residues) or $\pm\pi$ (positive or negative residue, respectively). The residue field for subscene 'A' of the Bathurst Island scene is shown in the last image panel of Figure 10. Although the residue field is comparatively sparse, it usually provides a better resolution map of certain phase discontinuities than either the coherence or the circular variance.

Conclusion

In temperate environments the shoreline is ideally defined by the interface between the relatively high coherence of the shore and the absence of coherence from the body of water. In practice, scene decorrelation from a variety of sources reduces, and often completely eliminates, coherence along the shore, thereby severely limiting the visibility of the shoreline in coherence maps. Similar factors reduce the difference in radar backscatter between the shore and the body of water. Both of these factors severely limit the practical use of the coherence map (either by itself or in conjunction with radar backscatter) for general use in shoreline extraction, though, under the right conditions, it can be accomplished.

The use of coherence for shoreline mapping and water body masking holds much more promise in arctic environments where decorrelation is minimised and the frozen water bodies and (frozen) land generally maintain a high coherence over a prolonged period of time. Under these circumstances, the coastline is often clearly outlined by a thin shear region of low coherence separating the two regions of higher coherence. This shear region is formed by the tidal induced change in the level of the sea ice relative with the fixed land. Small islands are also outlined by the same method. Volumetric scattering mechanism of Lake Ice results in higher interferogram phase noise over the lake, and a degradation in its coherence. This contrast nicely with, and can often be easily separated from, the higher coherence of the surrounding land.

The very requirement of a sampling window of pixels to estimate the coherence (or circular variance) limits, and indeed lowers, the coherence map's resolution relative to the inherent resolution of the radar backscatter image. This disadvantage can be addressed in several ways. The resolution of the coherence map can be improved by varying the size and shape of the estimation window or by using a multi-resolution coherence map. The lower resolution coherence map can be supplemented by the use of the readily available higher resolution radar backscatter image, interferogram phase, or residue images. The derivation of the coastline from the backscatter image can only approach an ideal of approximately one pixel r.m.s. (30m for ERS-1/2). In reality, the accuracy may be worse. A multi-temporal approach could also serve to increase not only the resolution of the scene, but information content as well.

References

1. J. Bruniquel and A. Lopes, "Multi-Variate Optimal Speckle Reduction in SAR Imagery," *Int. J. Remote Sensing*, vol. 18, no. 3, 1997.
2. P. Gineste, "Technical Note: A Simple, Efficient Filter for Multitemporal SAR Images," *Int. J. Remote Sensing*, vol. 20, no. 13, 1999.
3. F. Gatelli, A.M.Guarnieri, F. Parizzi, P.Pasquali, C. Prati and F. Rocca, "The wavenumber Shift in SAR Interferometry," *IEEE Trans. GRS*, vol. 32, no. 4, July 1994, pp. 855-865.
4. R.M. Goldstein, H.A. Zebker and C.L. Werner, "Satellite radar interferometry: two-dimensional phase unwrapping," *Radio Science*, vol. 23, 1988, pp. 713-20.
5. K.V. Mardia, "Statistics of Directional Data," New York: Academic Press, 1972.
6. K.E. Mattar, A.L. Gray, D. Geudtner and P.W. Vachon, "Interferometry for DEM and Terrain Displacement: Effects of Inhomogeneous Propagation," *Canadian Journal of Remote Sensing*, vol. 25, no. 1, March 1999, pp. 60-69.
7. P.A. Rosen, S.Hensley, I.R. Joughin, F.K. Li, S.N. Madsen, E. Rodriguez and R.M. Goldstein, "Synthetic Aperture Radar Interferometry," *Proc. IEEE*, vol. 88, no. 3, March 2000, pp.332-381.
8. M. Santoro *et al*, " Monitoring Urban Areas by Means of Coherence Levels", *ESA FRINGE '99 Conference Proceedings* (see http://www.esa.int/fringe99).
9. R. Scheiber and A. Moreira, "Coregistration of Interferometric SAR Images Using Spectral Diversity," *IEEE Trans. GRS*, vol 38, no 5, September 2000, pp. 2179-2190.
10. R. Touzi, A. Lopes, J. Bruniquel and P.W. Vachon, "Coherence Estimation for SAR Imagery," *IEEE Trans. GRS*, vol. 37, no. 1, January 1999, pp. 135-149.
11. H.A. Zebker and H.Villasenor, "Decorrelation in Interferometric Radar Echoes", *IEEE Trans. GRS*, vol. 30, no. 5, September 1992, pp. 950-959.

List of symbols/abbreviations/acronyms/initialisms

CFA	Center For Astrophysics
DEM	Digital Elevation Model
DTED	Digital Terrain Elevation Data
DND	Department of National Defence
DREO	Defence Research Establishment Ottawa
ERS	European Remote Sensing
ESA	European Space Agency
ESRIN	European Space Research Institute
GCP	Ground Control Point
GPS	Global Positioning System
ILU	Interferometric Land Use
InSAR	Interferometric SAR
LIDAR	Laser-Radar
MHWL	Mean High Water Level
NIMA	National Imagery Mapping Agency
SAR	Synthetic Aperture Radar
SLC	Single look complex
SRI	Satellite radar interferometry
SRTM	Shuttle Radar Topographic Mission
USGS	United Sates Geological Survey

DOCUMENT CONTROL DATA

(Security classification of title, body of abstract and indexing annotation must be entered when the overall document is classified)

1. ORIGINATOR (the name and address of the organization preparing the document. Organizations for whom the document was prepared, e.g. Establishment sponsoring a contractor's report, or tasking agency, are entered in section 8.)

DREO/ARN
3701 Carling Avenue
Ottawa, Ontario, Canada

2. SECURITY CLASSIFICATION (overall security classification of the document, including special warning terms if applicable)

UNCLASSIFIED

3. TITLE (the complete document title as indicated on the title page. Its classification should be indicated by the appropriate abbreviation (S,C or U) in parentheses after the title.)

Shoreline Mapping Using Interferometric SAR (U)

4. AUTHORS (Last name, first name, middle initial)

Mattar, Karim E., Buchheit, Max, Beaudoin, André

5. DATE OF PUBLICATION (month and year of publication of document)	6a. NO. OF PAGES (total containing information. Include Annexes, Appendices, etc.)	6b. NO. OF REFS (total cited in document)
October 2001	24	11

7. DESCRIPTIVE NOTES (the category of the document, e.g. technical report, technical note or memorandum. If appropriate, enter the type of report, e.g. interim, progress, summary, annual or final. Give the inclusive dates when a specific reporting period is covered.)

Technical report

8. SPONSORING ACTIVITY (the name of the department project office or laboratory sponsoring the research and development. Include the address.)

DREO/ARN

9a. PROJECT OR GRANT NO. (if appropriate, the applicable research and development project or grant number under which the document was written. Please specify whether project or grant)	9b. CONTRACT NO. (if appropriate, the applicable number under which the document was written)
5eb13	

10a. ORIGINATOR'S DOCUMENT NUMBER (the official document number by which the document is identified by the originating activity. This number must be unique to this document.)	10b. OTHER DOCUMENT NOS. (Any other numbers which may be assigned this document either by the originator or by the sponsor)
DREO TR 2001-078	

11. DOCUMENT AVAILABILITY (any limitations on further dissemination of the document, other than those imposed by security classification)

(x) Unlimited distribution
( ) Distribution limited to defence departments and defence contractors; further distribution only as approved
( ) Distribution limited to defence departments and Canadian defence contractors; further distribution only as approved
( ) Distribution limited to government departments and agencies; further distribution only as approved
( ) Distribution limited to defence departments; further distribution only as approved
( ) Other (please specify):

12. DOCUMENT ANNOUNCEMENT (any limitation to the bibliographic announcement of this document. This will normally correspond to the Document Availability (11). However, where further distribution (beyond the audience specified in 11) is possible, a wider announcement audience may be selected.)

13. ABSTRACT (a brief and factual summary of the document. It may also appear elsewhere in the body of the document itself. It is highly desirable that the abstract of classified documents be unclassified. Each paragraph of the abstract shall begin with an indication of the security classification of the information in the paragraph (unless the document itself is unclassified) represented as (S), (C), or (U). It is not necessary to include here abstracts in both official languages unless the text is bilingual).

Coherence from repeat-pass Satellite Radar Interferometry (SRI) is explored as a means for shoreline mapping and water body masking. In temperate environments the coast may be outlined by the difference between the high coherence of the land and the absence of coherence in the sea/ocean. However, it is found that in coastal regions scene decorrelation from a variety of sources often dominate the image, making it difficult or impossible to distinguish the shoreline. In an arctic climate where scene decorrelation is reduced and the sea is frozen, the shoreline is often clearly outlined by a thin region of low coherence separating the land from frozen ice that is subjected to continuous tidal shear forces. Lakes are similarly outlined by a reduction in the coherence.

14. KEYWORDS, DESCRIPTORS or IDENTIFIERS (technically meaningful terms or short phrases that characterize a document and could be helpful in cataloguing the document. They should be selected so that no security classification is required. Identifiers such as equipment model designation, trade name, military project code name, geographic location may also be included. If possible keywords should be selected from a published thesaurus. e.g. Thesaurus of Engineering and Scientific Terms (TEST) and that thesaurus-identified. If it is not possible to select indexing terms which are Unclassified, the classification of each should be indicated as with the title.)

InSAR, interferometry, SAR, shoreline masking, coastline masking, waterbody masking

Defence R&D Canada
is the national authority for providing
Science and Technology (S&T) leadership
in the advancement and maintenance
of Canada's defence capabilities.

R et D pour la défense Canada
est responsable, au niveau national, pour
les sciences et la technologie (S et T)
au service de l'avancement et du maintien des
capacités de défense du Canada.

DEFENCE R&D DÉFENSE

www.drdc-rddc.dnd.ca